HHS Public Access

Author manuscript

Oncogene. Author manuscript; available in PMC 2012 September 22.

Published in final edited form as:

Oncogene. 2012 March 22; 31(12): 1484–1492. doi:10.1038/onc.2011.339.

PP2A-B56α Controls Oncogene-Induced Senescence in Normal and Tumor Human Melanocytic Cells

Sudha Mannava[1], **Angela R. Omilian**[2], **Joseph A. Wawrzyniak**[1], **Emily E. Fink**[1], **Dazhong Zhuang**[1], **Jeffrey C. Miecznikowski**[4], **James R. Marshall**[3], **Maria S. Soengas**[5], **Rosalie C. Sears**[6], **Carl D. Morrison**[2], and **Mikhail A. Nikiforov**[1]

[1]Roswell Park Cancer Institute, Buffalo, New York, Department of Cell Stress Biology

[2]Roswell Park Cancer Institute, Buffalo, New York, Department of Pathology

[3]Roswell Park Cancer Institute, Buffalo, New York, Department of Cancer Prevention and Population Sciences

[4]Roswell Park Cancer Institute, Buffalo, New York, Department of Biostatistics

[5]Spanish National Cancer Research Center, Madrid, Spain

[6]Oregon Health and Science University, Oregon, USA

Abstract

Oncoprotein C-MYC is overexpressed in human metastatic melanomas and melanoma-derived cells where it is required for suppression of oncogene-induced senescence (OIS). The genetic events that maintain high levels of C-MYC in melanoma cells and their role in OIS are unknown. Here, we report that C-MYC in cells from several randomly chosen melanoma lines was up-regulated at the protein level, and largely due to the increased protein stability. Of all known regulators of C-MYC stability, levels of B56α subunit of the PP2A tumor suppressor complex were substantially suppressed in all human melanoma cells compared to normal melanocytes. Accordingly, immuno-histochemical analysis revealed that the lowest and the highest amounts of PP2A-B56α were predominantly detected in metastatic melanoma tissues and in primary melanomas from patients with good clinical outcome, respectively. Importantly, PP2A-B56α overexpression suppressed C-MYC in melanoma cells and induced OIS, whereas depletion of PP2A-B56α in normal human melanocytes up-regulated C-MYC protein levels and suppressed $BRAF^{V600E}$- and, less efficiently, $NRAS^{Q61R}$-induced senescence. Our data reveal a mechanism of C-MYC overexpression in melanoma cells and identify a functional role for PP2A-B56α in OIS of melanocytic cells.

Corresponding Author: Mikhail A. Nikiforov, Roswell Park Cancer Institute, Department of Cell Stress Biology, BLSC L3-317, Elm & Carlton Streets, Buffalo, NY, 14263. Phone: 716-845-3374; FAX: 716-845-3944; Mikhail.nikiforov@roswellpark.org.

Conflict of interest

The authors declare no conflict of interest.

Keywords

PP2A-B56α; C-MYC; melanoma; senescence

Introduction

Oncogene-induced senescence (OIS) is a mechanism for the suppression of tumor growth at the pre-neoplastic stage (Bringold and Serrano, 2000; Mooi and Peeper, 2006; Bansal and Nikiforov, 2010). One of the best examples of naturally occurring OIS in humans is the nevus, a benign aggregation of non-proliferative melanocytes that often harbor activating mutations in *BRAF*, *NRAS* or *HRAS* genes (Michaloglou *et al.*, 2005; Gray-Schopfer *et al.*, 2007; Pollock *et al.*, 2003). Intriguingly, activating mutations in the same genes have been detected in several types of malignant melanomas but at lower frequencies (Pollock *et al.*, 2003; Curtin *et al.*, 2005; Maldonado *et al.*, 2003), indicating that malignant melanomas that often originate from nevi must have developed mechanisms that circumvent OIS. Ectopic expression of the activated forms of the above oncogenes ($BRAF^{V600E}$, $NRAS^{Q61R}$, $HRAS^{G12V}$) in normal human melanocytes (NHM) also induced senescence (Pollock *et al.*, 2003; Denoyelle *et al.*, 2006) which was not prevented by individual depletion of such tumor suppressor genes as p53, $p16^{INK4A}$ (Denoyelle *et al.*, 2006; Zhuang *et al.*, 2008), $p21^{CIP/WAF}$ or $p14^{ARF}$ (Haferkamp *et al.*, 2009). Instead, ectopic expression of the oncogenic transcription factor C-MYC has been shown to significantly suppress senescence phenotypes caused by $BRAF^{V600E}$ and, to much lesser extent, by $NRAS^{Q61R}$ in NHM (Zhuang *et al.*, 2008).

C-MYC is a member of the MYC family of oncoproteins (Grandori *et al.*, 2003; Nikiforov *et al*, 2003). It regulates the expression of more than 3,000 genes involved in a large variety of cellular processes including the cell cycle regulation (Henriksson and Lüscher, 1996), differentiation (Eilers, 1999), metabolism (Dang and Gao, 2009; Mannava *et al.*, 2008), apoptosis (Nilsson and Cleveland, 2003; Meyer *et al.*, 2006) and senescence (Wu *et al.*, 2007; Zhuang *et al.*, 2008; Hydbring et al, 2010). C-MYC is required for the proliferation of all tested human cells (Wang *et al.*, 2008) and is frequently up-regulated in human malignancies including metastatic melanoma (Nesbit *et al.*, 1999). In cells from solid tumors, the elevated expression of C-MYC can be maintained through several mechanisms including gene amplification (Nesbit *et al.*, 1999), enhanced cap-dependent and cap-independent translation of *C-MYC* mRNA (De Benedetti *et al.*, 2004; Shi *et al.*, 2008) and elevated protein stability (Hann, 2006). C-MYC stability is regulated in part by post-translational modifications on its two highly conserved residues: phosporylation of Ser^{62} by the RAS-RAF-MEK-ERK kinase cascade stabilizes C-MYC (Lutterbach and Hann, 1994; Sears *et al.*, 1999), whereas phopshorylation of Thr^{58} by GSK3β kinase promotes C-MYC proteosomal degradation (Gregory and Hann, 2000; Bahram *et al.*, 2000). C-MYC phosphorylated on Thr^{58} is recognized by FBW7, a receptor component of the ubiquitin-ligase complex SCF (Skp2-Cullin-F-box), and is subsequently ubiquitinated (Kim *et al.*, 2003; Welcker *et al.*, 2004). MYC phosphorylated at Ser^{62}/Thr^{58} is also recognized by the prolylisomerase Pin1 that induces conformational changes at the peptide bond between Ser^{62} and Pro^{63} and facilitates interactions between phosphorylated Ser^{62} and a serine/

threonine phosphatase complex PP2A (Arnold and Sears, 2006). PP2A dephosphorylates phospho-Ser^{62} of C-MYC thus promoting its degradation. PP2A consists of a structural subunit (A), catalytic subunit (C), and one of multiple regulatory subunits (B) that specify PP2A target binding (Arroyo and Hann, 2005). The B56α regulatory subunit of PP2A has been shown to interact with C-MYC, enhance dephosphorylation of phospho-Ser^{62} and promote C-MYC degradation (Arnold and Sears, 2006). Depletion of PP2A-B56α cooperated with SV40 T antigen, catalytic subunit of telomerase reverse transcriptase and HRAS^{G12V} in transformation of human kidney epithelial cells (Sablina *et al.*, 2010). Yet, unlike other protein controlling C-MYC stability (Rajagopalan *et al.*, 2004; Vaarala *et al.*, 2010), deregulated expression of PP2A-B56α has never been associated with any human malignancies.

Other proteins regulating C-MYC stability include: CIP2A, a C-MYC-interacting protein that specifically inhibits PP2A activity against C-MYC (Junttila *et al.*, 2007); USP28, a de-ubiquitinating enzymes that antagonizes FBW7 and promotes C-MYC stability (Popov *et al.*, 2007) and TRUSS, a receptor for DDB1 (damage-specific DNA-binding protein 1)-CUL4 (Cullin 4) E3 ligase complex (Choi *et al.*, 2010).

Recently, we have demonstrated that shRNA-mediated depletion of C-MYC in metastatic melanoma cells resulted in the re-emergence of senescence phenotypes that were characteristic for NHM ectopically expressing BRAF^{V600E} or NRAS^{Q61R} (Zhuang *et al.*, 2009). The mechanisms maintaining high levels of C-MYC in melanoma cells and their role in suppression of OIS remain unknown. To answer this question, we report here that increased protein stability plays a major role in maintaining high amounts of C-MYC in melanoma cells and that PP2A-B56α represents a key regulator of C-MYC protein stability and oncogene-induced senescence in normal and transformed melanocytic cells.

Results

C-MYC abundance in human melanoma cells is maintained at the protein level

To investigate mechanisms underlying overexpression of C-MYC in melanoma cells, we analyzed C-MYC protein and mRNA levels in cells from seven arbitrarily chosen melanoma lines derived from human melanoma metastases and two independently isolated populations of NHM. C-MYC protein levels were ~ 4 to 11 times higher in melanoma cells compared to NHM (Figure 1a), whereas C-MYC mRNA amounts in melanoma cells were at most 2.5 fold higher than that of NHM (Figure 1b). These data suggest that high amounts of C-MYC in studied melanoma cells could be due to the increased protein stability or elevated translational rates of its mRNA. To test the former possibility, C-MYC protein half-life was assessed in a population of NHM (designated as “b” on Figure 1a) and in cells from 3 arbitrary chosen melanoma cell lines, SK-Mel-19, SK-Mel-29, SK-Mel-147, in pulse-chase ^{35}S-methionine/cysteine labeling assay. As shown in Figure 1c, C-MYC protein half-life was 2.6 to 7.3 fold higher in melanoma cells than in NHM indicating that C-MYC protein is more stable in melanoma cells compared to NHM.

Several polypeptides were implicated in the control of C-MYC protein stability: PP2A-B56α, PP2A-C, FBW7–α,–β,–γ; PIN1, SKP2, CIP2A, TRUSS and USP28. We examined

the expression of these polypeptides in NHM and melanoma cells by Western blotting. Surprisingly, expression of only two of these proteins, PP2A-B56α and CIP2A, differed dramatically between NHM and all melanoma cells (Figure 2a). PP2A-B56α, was acutely suppressed in melanoma cells compared to NHM, whereas CIP2A demonstrated directly the opposite expression pattern. Interestingly, the expression of PP2A-C, a catalytic subunit of PP2A complex, did not change among the studied cells.

CIP2A has been recently characterized as a direct target of C-MYC gene (Khanna *et al.*, 2009), whereas ability of C-MYC to regulate PP2A-B56α has never been investigated. To address this question, we depleted C-MYC in cells from two arbitrarily chosen melanoma lines via shRNA (Wang *et al.*, 2008) and monitored expression of CIP2A and PP2A-B56α by Western blotting 6 days post-infection. Depletion of C-MYC substantially affected levels of CIP2A but not PP2A-B56α (Figure 2b) indicating that PP2A-B56α expression does not depend on C-MYC in studied melanoma cells.

To validate the expression pattern of PP2A-B56α observed in cultured cells, we analyzed its protein levels immunohistochemically in tissue microarrays (TMAs) containing 56 primary cutaneous melanomas from the individuals with good clinical outcome (in lieu of TMA containing adequate number of samples from benign melanocytic nevi) and 167 metastatic melanoma specimens (Table 1). Our analysis revealed a significant correlation between intensity of PP2A-B56α staining and tumor stage (Somers' D statistic = −0.2046, p-value = 0.0036). Specifically, cores with the highest expression of PP2A-B56α (intensity score 3; more than 50% of cells stained) were 12.22 times more frequent in TMAs derived from primary tumors compared to metastases (p=0.0237), whereas cores with the lowest expression of PP2A-B56α (intensity score 0) were 3.71 times more likely to be derived from metastatic samples than primary tumors (p=0.0242). Representative cores from each group are shown in Figure 2c. These results confirm our observations made in cultured cells that PP2A-B56α is down-regulated during melanoma progression.

PP2A-B56α suppresses C-MYC in melanoma cells and induces senescence-like phenotypes

To determine whether PP2A-B56α affects C-MYC in melanoma cells, the cells from 4 melanoma lines were infected with a lentiviral vector encoding PP2A-B56α or empty vector. Ectopic expression of PP2A-B56α in SK-Mel-19 and SK-Mel-29 cells caused substantial down-regulation of C-MYC protein amounts and proliferative arrest between days 5 and 8 post-infection (Figure 3ac). Proliferation arrest was accompanied by increased activity of SA-β-Gal (Figure 3ad). SK-Mel-103 and -147 cells expressing ectopic PP2A-B56α underwent proliferative arrest at later time point, between days 14 and 20 post-infection (Figure 3c). Like in SK-Mel-19 and -29 cells, the arrest was accompanied by decrease in C-MYC amounts (Figure 3a) and increased activity of SA-β-Gal compared to control cells (Figure 3d). It is noteworthy that in cells from all lines the senescence-associated phenotypes induced by PP2A-B56α overexpression were very similar to those caused by direct depletion of C-MYC via shRNAs (Zhuang *et al.*, 2008). Therefore ectopic expression of PP2A-B56α induces senescence in melanoma cells, albeit with different incubation period. Importantly, overexpression of PP2A-B56α in cells from 3 out of 4 tested

lines (SK-Mel-19, -29, and -147) either did not affect C-MYC mRNA levels or depleted them roughly by ~50% (Figure 3b), demonstrating that PP2A-B56α controls C-MYC in melanoma cells predominantly at the protein level.

Depletion of PP2A-B56α in NHM leads to increased C-MYC levels and resistance to $BRAF^{V600E}$-induced senescence and partial resistance to $NRAS^{Q61R}$-induced senescence

To identify whether C-MYC protein levels depend on endogenous PP2A-B56α, we infected NHM with lentiviral vectors containing two different shRNAs against PP2A-B56α or control shRNA. Cells were collected 5 days post-infection to assess changes in C-MYC and PP2A-B56α mRNA and protein levels. Each shRNA against PP2A-B56α efficiently depleted its mRNA and protein (Figure 3ef). Importantly, PP2A-B56α depletion resulted in 3.1-to-3.4-fold increase in the amounts of C-MYC protein, but not mRNA (Figure 3ef).

As B56α controls PP2A-dependent de-phosphorylation of C-MYC phospho-Ser^{62}, we investigated the effect of shRNA-mediated depletion of PP2A-B56α on this modification of C-MYC. Using Western blotting with antibodies specific to total or phospho-Ser^{62} C-MYC, we detected an ~50% increase in C-MYC protein phosphorylated on Ser^{62} in PP2A-B56α-depleted cells (Figure 3e), thus providing a mechanistic explanation to the increased C-MYC protein amounts.

To identify whether PP2A-B56α depletion overcomes OIS in NHM, first, these cells were infected with lentiviral vector expressing $BRAF^{V600E}$ or with empty lentiviral vector followed by super-infection with control or PP2A-B56α shRNAs. The functional activity of $BRAF^{V600E}$ in infected cells was confirmed by monitoring phosphorylation of ERK, a downstream target of activated RAS-RAF pathway (Figure 4a). As has been shown previously (Zhuang *et al.*, 2008), a significant decline in C-MYC amounts was observed in $BRAF^{V600E}$-expressing melanocytes between days 10 and 15 post-infection (Figure 4b), concomitant with the strong manifestation of the senescence-associated phenotypes including reduction in proliferative rates (assessed by the EdU incorporation) and the increase in the percentage of SA-β-Gal-positive cells and cells containing senescence-associated heterochromatin foci (SAHF) (Figure 4cd). Depletion of PP2A-B56α in $BRAF^{V600E}$-expressing melanocytes prevented downregulation of C-MYC and the emergence of senescence-associated phenotypes (Figure 4b–d). These data demonstrate that suppression of PP2A-B56α has a functional role in overcoming $BRAF^{V600E}$-induced senescence most likely via sustaining endogenous C-MYC levels. Recently, we have demonstrated that C-MYC overexpression in NHM overcomes $BRAF^{V600E}$-induced more effectively than $NRAS^{Q61R}$-induced senescence To address the role of PP2A-B56α in OIS induced by activated members of RAS protein family that commonly mutate in melanocytic cells, we suppressed PP2A-B56α in NHM followed by transduction with $NRAS^{Q61R}$ or $HRAS^{G12V}$-expressing lentiviruses. The activities of infected RAS proteins were confirmed by monitoring phosphorylation of ERK (Figure 4a). Depletion of PP2A-B56α reversed downregulation of C-MYC caused by $NRAS^{Q61R}$ or $HRAS^{G12V}$ almost as efficiently as in case with $BRAF^{V600E}$ (Figure 4b). Interestingly, upregulation of C-MYC partially reversed senescence-associated phenotypes caused by $NRAS^{Q61R}$ but did not significantly suppress these phenotypes induced by $HRAS^{G12V}$ (Figure 4cd).

Thus, in NHM, PP2A-B56α depletion differentially affects OIS induced by members of RAS family of proteins most commonly activated in melanocytic cells.

Discussion

In the current manuscript, we present data arguing that protein stability is a major factor contributing to the elevated levels of C-MYC in melanoma cells. Furthermore, we demonstrate that among all known regulators of C-MYC stability, the expression of two proteins that regulate PP2A activity against C-MYC (CIP2A and PP2A-B56α) were markedly different between NHM and melanoma cells. Therefore, it is quite remarkable that despite high genetic variability of melanoma cells (Smalley *et al.*, 2005), C-MYC was similarly up-regulated in cells from all studied melanoma lines and that the expression of two proteins regulating a single post-translational modification of C-MYC (phosphorylation of Ser^{62}) was also respectively uniformed among these lines. In principal, this uniformity could be due to another feature common for all studied melanoma cells: the activated state of MEK-ERK pathway. Because Ser^{62} is a target of ERK (Sears *et al*, 1999), phosphorylation of Ser^{62} can be a rheostat for the opposing activities of ERK and PP2A.

Activation of BRAF, NRAS or HRAS plays a controversial role in melanomagenesis. On the one hand, constitutive activity of these oncoproteins is essential for sustained proliferation of melanoma cells which requires high levels of C-MYC (Zhuang *et al.*, 2008; Welcker *et al.*, 2004). On the other hand, these oncogenes cause OIS in NHM accompanied by down-regulation of C-MYC (Zhuang *et al.*, 2008). Intriguingly, $BRAF^{V600E}$ stimulates proliferation shortly after delivery into NHM and suppresses it at later time points (Denoyelle *et al.*, 2006; Zhuang *et al.*, 2008). Our previous and current data support the model that suppression of C-MYC is responsible for the transition from proliferation-promoting to proliferation-inhibitory activities of $BRAF^{V600E}$ and possibly activated RAS proteins.

We report that overexpression of PP2A-B56α suppressed C-MYC protein rather than mRNA levels in cells from two out of four examined melanoma lines. In the other two lines (SK-Mel-19 and SK-Mel-103), PP2A-B56α overexpression led to 50% and 77% reduction in *C-MYC* mRNA, respectively. This phenomenon may be due to the reported ability of PP2A-B56α to facilitate degradation of β-catenin (Arnold *et al.*, 2009; Hart *et al.*, 1998), a mediator of Wnt-pathway-dependent up-regulation of *C-MYC* transcription (He *et al.*, 1998). Because the Wnt pathway is often activated in melanoma cells (Larue and Delmas, 2006) including SK-Mel-103 (D.Z. and M.A.N. unpublished observations), the presumed degradation of β-catenin via PP2A-B56α in these cells may affect *C-MYC* mRNA levels.

PP2A-B56α-dependent depletion of C-MYC in studied melanoma cells resulted in the emergence of senescence phenotypes similar to those caused by depletion of C-MYC via shRNA. However, the timing of senescence varied substantially: 5–6 days post-infection with PP2A-B56α in SK-Mel-19, -29 cells versus 14–20 days post-infection in SK-Mel-103, -147 cells. In the latter group, the amounts of C-MYC did not change until prior to the emergence of senescence phenotypes (data not shown), indicating that ectopic PP2A-B56α in these cells did not suppress C-MYC amounts during a long period of time. One possible

explanation for this observation is that unlike $BRAF^{V600E}$-expressing SK-Mel-19 and SK-Mel-29 cells that contain activated ERK (Figure 1a), SK-Mel-103 and SK-Mel-147 cells bear $NRAS^{Q61R}$ and, therefore possess both activated ERK and suppressed GSK3β. This leads to stabilization of C-MYC by increased phosporylation of its Ser^{62} and hypo-phosphorylation of its Thr^{58} Therefore, it is conceivable that destabilization of C-MYC in SK-Mel-103 and SK-Mel-147 cells *via* PP2A-mediated de-phosphorylation of Ser^{62} is hampered or delayed compared to that in SK-Mel-19 and -29 cells.

Depletion of PP2A-B56α led to the up-regulation of endogenous C-MYC in NHM expressing $BRAF^{V600E}$, $NRAS^{Q61R}$ or $HRAS^{G12V}$. Yet, C-MYC increase was sufficient to effectively suppress senescence phenotypes caused only by $BRAF^{V600E}$. OIS induced by $NRAS^{Q61R}$ was inhibited only partially, whereas $HRAS^{G12V}$-dependent senescence phenotypes were unaffected by upregulation of C-MYC. These data are concordant with our previous observations that ectopic expression of C-MYC much more efficiently overcomes OIS caused by $BRAF^{V600E}$ than by $NRAS^{Q61R}$ (Zhuang *et al.*, 2008). Unlike $BRAF^{V600E}$, $HRAS^{G12V}$ and, to much lesser extent, $NRAS^{Q61R}$ induce the unfolded protein response (UPR) in NHM (Denoyelle *et al.*, 2006). In our experience, C-MYC overexpression in NHM does not suppress the UPR pathway (Zhuang *et al.*, 2008), which could account for the inability of PP2A-B56α depletion and subsequent C-MYC up-regulation to overcome $HRAS^{G12V}$-induced senescence in these cells.

In summary, we demonstrated that increased protein stability contributes substantially to the elevated levels of C-MYC in melanoma cells. We showed that PP2A-B56α can account for differential C-MYC expression between NHM and melanoma cells. Lastly, we demonstrated the functional importance of PP2A-B56α downregulation for both the maintenance of high levels of C-MYC and the suppression of oncogene-induced senescence in NHM and melanoma cells.

Materials and methods

Cell lines

Melanoma cell lines were originally obtained from Memorial Sloan Kettering Cancer Center. Cells were cultured in Dulbecco's modified Eagle's essential minimal medium as recommended by the supplier. Supplements included fetal calf serum (10%), 2 mM glutamine, and 100 units/ml penicillin G + 100 μg/ml streptomycin. All cell culture agents were purchased from Invitrogen, Inc. (Carlsbad, CA). Normal melanocytes were isolated from neonatal foreskins as previously described (8) and maintained in Medium 254 supplemented with 0.2 mM CaCl2, 16 nM TPA and melanocyte growth factors (Cascade Biologics).

Assays for cell proliferation and senescence

For the proliferation assay, melanocytes were plated in 96 well plates at ~50% confluence 2 days prior to the assay. Cells were incubated with a nucleoside analog of thymidine, 5-ethynyl-2´-deoxyuridine (EdU), for 60 minutes followed by fixation and staining for EdU-incorporated cells using the ClickiT™ EdU Assay kit (Invitrogen). The proportion of EdU-

positive cells was determined by counting cells under the fluorescent microscope in multiple view fields.

For the senescence assay, cells were plated in 12 well plates at ~30% confluence 2 days prior to the assay. Cells were fixed and incubated for different time periods (4 hours to overnight, depending on the cell line) at 37°C with the staining solution containing the X-Gal substrate (BioVision). The development of blue color was detected visually with a microscope. The proportion of positive cells was determined by counting cells under the light microscope in multiple view fields. To visualize senescence-associated heterochromatin foci (SAHF), cells were fixed with 0.5% formaldehyde and stained with DAPI as described previously (Denoyelle *et al.*, 2006). The proportion of SAHF-positive cells was determined by counting cells with fluorescent microscopy in multiple view fields.

Assay for C-MYC protein stability

C-MYC protein stability was determined using pulse-chase labeling with ^{35}S-methionine/^{35}S-cysteine. NHM and melanoma cells were pulse-labeled with the mixture of ^{35}S-methionine/^{35}S-cysteine (300μCi/ml, Perkin-Elmer) in the cysteine- and methionine-free media for 3 hours and 1 hour, respectively. After that, cells were washed and incubated in media containing non-radioactive cysteine and methionine for 0, 20, 40 or 60 minutes. After completion of incubation, cells were harvested, lysed in immunoprecipitation buffer and total cellular extracts were immunoprecipitated with mouse anti-C-MYC monoclonal antibodies (C33, SantaCruz). Immunoprecipitated materials were separated on 10% SDS-PAGE, and labeled C-MYC was quantified using STORM phospho-imager.

Lentiviral constructs and infection

Lentiviral infection protocols and vectors containing control shRNA, C-MYC shRNA, cDNAs of BRAF^{V600E}, NRAS^{Q61R} and HRAS^{G12V} were described previously (Denoyelle *et al.*, 2006; Arnold and Sears, 2006). The pLKO-1 lentiviral vectors containing shRNAs specific for the human gene encoding PP2A-B56α were purchased from Sigma.

Quantitative Reverse Transcription Real-Time PCR (Q-RT-PCR)

Total RNA was isolated from cells using the RNeasy Mini Kit (Qiagen). cDNA was prepared using the cDNA reverse transcription kit (Invitrogen). Q-RT-PCR was performed on 7900HT Fast Real-Time PCR System (Applied Biosystems) using TaqMan® Universal Master Mix II (Applied Biosystems) and probes and PCR primers specific for human β-actin, human C-MYC or human PP2A-B56α genes. PCR data were analyzed using sequence detection software (SDS) 2.4 (Applied Biosystems).

Immunoblotting and immunofluorescence

Antibodies were used against the following human proteins: p53, C-MYC, SKP2, CIP2A, ERK1/2 and ERK1/2-γ from Santa Cruz Biotechnology (sc-99, sc-42, sc-7164, sc-80659, sc-93, sc-7383, respectively); C-MYC-Ser-62, PP2A-B56α and Fbw7 from Abcam (ab78318, ab1084 and ab12292, respectively); p16^{INK4A} PIN1, USP28, from Cell Signaling Technology (4824, 3722, 4217s); from SPP2A-C from BD Bioscience (bd-610555); and TRUSS from Proteintech (12606-1-AP). Membranes were developed using alkaline

phosphatase-conjugated secondary antibodies and the Alpha-Innotech FluorChem HD2® imaging system. Quantification of the signal was performed using the ImageQuant 2.0 program package. The background was calculated from an equivalent area in each lane and subtracted from the value for the protein signal in that lane.

Tissue microarrays (TMAs), immunohistochemistry and statistical analysis

Three 1-millimeter tissue cores of formalin-fixed and paraffin-embedded primary cutaneous tissue from patients with good prognosis (56 cores) or metastatic melanoma (167 cores) were precisely arrayed into paraffin blocks. Immunohistochemical (IHC) staining was performed using the PP2A-B56α mouse monoclonal antibody (clone 23/B56α; BD Biosciences; dilution 1:50). Briefly, this procedure consisted of deparaffinization and rehydration followed by epitope retrieval in which the tissue microarrays were immersed in Target Retrieval Solution (Dako) and incubated with steam for 40 minutes. Incubation with PP2A-B56α antibodies was performed for 45 minutes and was followed by the serial application of biotinylated goat anti-mouse IgG (Jackson ImmunoResearch), alkaline phosphatase-conjugated streptavidin (Invitrogen), and the Fast-Red Substrate System (Dako). Results were recorded as semi-quantitative/ordered categorical, according to the American Society of Clinical Oncology Guideline Recommendations. The neoplastic cells for any given core were scored for i) intensity of staining using the following scale: no staining (0), weak staining (1), moderate staining (2), strong staining (3). The Somers' D statistic (Newson, 2006) was used to assess the correlation between the intensity of immunohistochemical staining and tumor stage (primary or metastatic).

Acknowledgements

We are grateful to Dr. Catherine Burkhart (Cleveland Biolabs) and Dr. Shoshanna Zucker (Roswell Park Cancer Institute) for critical reading of the manuscript, Ms. Carina Fung (University of Sydney) for the experimental help. This work was supported by NIH R01 CA120244 and ACS RSG-10-121-01 grants to M.A.N. The work of J.C.M. was supported in part by the NIH 5P30CA016056-34 grant.

References

Arnold HK, Sears RC. Protein phosphatase 2A regulatory subunit B56α associates with c-myc and negatively regulates c-myc accumulation. Mol cell Biol. 2006; 26:2832–2844. [PubMed: 16537924]

Arnold HK, Zhang X, Daniel CJ, Tibbitts D, Escamilla-Powers J, Farrell A, et al. The Axin1 scaffold protein promotes formation of a degradation complex for c-Myc. EMBO J. 2009; 28:500–512. [PubMed: 19131971]

Arroyo JD, Hahn WC. Involvement of PP2A in viral and cellular transformation. Oncogene. 2005; 24:7746–7755. [PubMed: 16299534]

Bahram F, von der Lehr N, Cetinkaya C, Larsson LG. c-Myc hot spot mutations in lymphomas result in inefficient ubiquitination and decreased proteasome-mediated turnover. Blood. 2000; 95:2104–2110. [PubMed: 10706881]

Bansal R, Nikiforov MA. Pathways of oncogene-induced senescence in human melanocytic cells. Cell Cycle. 2010; 9:2782–2788. [PubMed: 20676024]

Bringold F, Serrano M. Tumor suppressors and oncogenes in cellular senescence. Exp Gerontol. 2000; 35:317–329. [PubMed: 10832053]

Choi SH, Wright JB, Gerber SA, Cole MD. Myc protein is stabilized by suppression of a novel E3 ligase complex in cancer cells. Genes Dev. 2010; 24:1236–1241. 2010. [PubMed: 20551172]

Curtin JA, Fridlyand J, Kageshita T, Patel HN, Busam KJ, Kutzner H, et al. Distinct sets of genetic alterations in melanoma. N Engl J Med. 2005; 353:2135–2147. [PubMed: 16291983]

Dang CV, Le A, Gao P. MYC-induced cancer cell energy metabolism and therapeutic opportunities. Clin Cancer Res. 2009; 15:6479–6483. [PubMed: 19861459]

De Benedetti A, Graff JR. eIF-4E expression and its role in malignancies and metastases. Oncogene. 2004; 23:3189–3199. [PubMed: 15094768]

Denoyelle C, Abou-Rjaily G, Bezrookove V, Verhaegen M, Johnson TM, Fullen DR, et al. Anti-oncogenic role of the endoplasmic reticulum differentially activated by mutations in the MAPK pathway. Nat Cell Biol. 2006; 8:1053–1063. [PubMed: 16964246]

Eilers M. Control of Cell proliferation by Myc family genes. Mol Cells. 1999; 9:1–6. [PubMed: 10102563]

Grandori C, Wu KJ, Fernandez P, Ngouenet C, Grim J, Clurman BE, et al. Werner syndrome protein limits MYC-induced cellular senescence. Genes Dev. 2003; 17:1569–1574. [PubMed: 12842909]

Gray-Schopfer V, Wellbrock C, Marais R. Melanoma biology and new targeted therapy. Nature. 2007; 445:851–857. [PubMed: 17314971]

Gregory MA, Hann SR. c-Myc Proteolysis by the Ubiquitin-Proteasome Pathway: Stabilization of c-Myc in Burkitt's Lymphoma Cells. Mol Cell Biol. 2000; 20:2423–2435. [PubMed: 10713166]

Hann SR. Role of post-translational modifications in regulating c-Myc proteolysis, transcriptional activity and biological function. Semin Cancer Biol. 2006; 216:288–302. [PubMed: 16938463]

Haferkamp S, Tran SL, Becker TM, Scurr LL, Kefford RF, Rizos H. The relative contributions of the p53 and pRb pathways in oncogene-induced melanocyte senescence. Aging. 2009; 1:542–556. [PubMed: 20157537]

Hart MJ, de los Santos R, Albert IN, Rubinfeld B, Polakis P. Downregulation of beta-catenin by human Axin and its association with the APC tumor suppressor, beta-catenin and GSK3 beta. Curr biol. 1998; 8:573–581. [PubMed: 9601641]

He TC, Sparks AB, Rago C, Hermeking H, Zawel L, da Costa LT, et al. Identification of c-MYC as a Target of the APC Pathway. Science. 1998; 281:1509–1512. [PubMed: 9727977]

Henriksson M, Lüscher B. Proteins of the Myc network: essential regulators of cell growth and differentiation. Adv Cancer Res. 1996; 68:109–182. [PubMed: 8712067]

Hydbring P, Bahram F, Su Y, Tronnersjö S, Högstrand K, von der Lehr N, Sharifi HR, Lilischkis R, Hein N, Wu S, Vervoorts J, Henriksson M, Grandien A, Lüscher B, Larsson LG. Phosphorylation by Cdk2 is required for Myc to repress Ras-induced senescence in cotransformation. Proc Natl Acad Sci U S A. 2010; 107:58–63. [PubMed: 19966300]

Junttila MR, Puustinen P, Niemelä M, Ahola R, Arnold H, Böttzauw T, et al. CIP2A inhibits PP2A in human malignancies. Cell. 2007; 130:51–62. [PubMed: 17632056]

Khanna A, Böckelman C, Hemmes A, Junttila MR, Wiksten JP, Lundin M, et al. MYC-dependent regulation and prognostic role of CIP2A in gastric cancer. J Natl Cancer Inst. 2009; 101:793–805. [PubMed: 19470954]

Kim SY, Herbst A, Tworkowski KA, Salghetti SE, Tansey WP. Skp2 regulates Myc protein stability and activity. Mol Cell. 2003; 11:1177–1188. [PubMed: 12769843]

Larue L, Delmas V. The WNT/Beta-catenin pathway in melanoma. Front Biosci. 2006; 11:733–742. [PubMed: 16146765]

Lopez-Bergami P, Fitchman B, Ronai Z. Understanding Signaling Cascades in Melanoma. Photochem Photobiol. 2008; 84:289–306. [PubMed: 18086245]

Lutterbach B, Hann SR. Hierarchical phosphorylation at N-terminal transformation-sensitive sites in c-Myc protein is regulated by mitogens and in mitosis. Mol Cel Biol. 1994; 14:5510–5522.

Maldonado JL, Fridlyand J, Patel H, Jain AN, Busam K, Kageshita T, et al. Determinants of BRAF mutations in primary melanomas. J Natl Cancer Inst. 2003; 95:1878–1890. [PubMed: 14679157]

Mannava S, Grachtchouk V, Wheeler LJ, Im M, Zhuang D, Slavina EG, et al. Direct role of nucleotide metabolism in C-MYC-dependent proliferation of melanoma cells. Cell Cycle. 2008; 7:2392–2400. [PubMed: 18677108]

Meyer N, Kim SS, Penn LZ. The Oscar-worthy role of Myc in apoptosis. Semin Cancer Biol. 2006; 16:275–287. [PubMed: 16945552]

Michaloglou C, Vredeveld LC, Soengas MS, Denoyelle C, Kuilman T, van der Horst CM, et al. BRAFE600-associated senescence-like cell cycle arrest of human naevi. Nature. 2005; 436:720–724. [PubMed: 16079850]

Mooi WJ, Peeper DS. Oncogene-induced cell senescence-halting on the road to cancer. N Engl J Med. 2006; 355:1037–1046. [PubMed: 16957149]

Nesbit CE, Tersak JM, Prochownik EV. MYC oncogenes and human neoplastic disease. Oncogene. 1999; 18:3004–3016. [PubMed: 10378696]

Newson R. Confidence intervals for rank statistics: Somers' D and extensions. The Stata J. 2006; 2:45–64.

Nikiforov MA, Popov N, Kotenko I, Henriksson M, Cole MD. The Mad and Myc basic domains are functionally equivalent. J.Biol.Chem. 2003; 278(110):94–11099.

Nilsson JA, Cleveland JL. Myc pathways provoking cell suicide and cancer. Oncogene. 2003; 22:9007–9021. [PubMed: 14663479]

Pollock PM, Harper UL, Hansen KS, Yudt LM, Stark M, Robbins CM, et al. High frequency of BRAF mutations in nevi. Nat Genet. 2003; 33:19–20. [PubMed: 12447372]

Popov N, Wanzel M, Madiredjo M, Zhang D, Beijersbergen R, Bernards R, et al. The ubiquitin-specific protease USP28 is required for MYC stability. Nat Cell Bbiol. 2007; 9:765–774.

Rajagopalan H, Jallepalli PV, Rago C, Velculescu VE, Kinzler KW, Vogelstein B, et al. Inactivation of hCDC4 can cause chromosomal instability. Nature. 2004; 428:77–81. [PubMed: 14999283]

Sablina AA, Hector M, Colpaert N, Hahn WC. Identification of PP2A Complexes and Pathways Involved in Cell Transformation. Cancer Res. 2010; 70:10474–10484. [PubMed: 21159657]

Sears R, Leone G, DeGregori J, Nevins JR. Ras enhances Myc protein stability. Mol Cell. 1999; 3:169–179. [PubMed: 10078200]

Shi Y, Frost PJ, Hoang BQ, Benavides A, Sharma S, Gera JF, et al. IL-6-induced stimulation of c-myc translation in multiple myeloma cells is mediated by myc internal ribosome entry site function and the RNA-binding protein, hnRNP A1. Cancer Res. 2008; 68:10215–10222. [PubMed: 19074889]

Smalley KS, Brafford PA, Herlyn M. Selective evolutionary pressure from the tissue microenvironment drives tumor progression. Semin Cancer Biol. 2005; 15:451–459. [PubMed: 16043361]

Vaarala MH, Väisänen MR, Ristimäki A. CIP2A expression is increased in prostate cancer. J Exp Clin Cancer Res. 2010; 29:136–140. [PubMed: 20964854]

Wang H, Mannava S, Grachtchouk V, Zhuang D, Soengas MS, Gudkov AV, et al. c-Myc depletion inhibits proliferation of human tumor cells at various stages of the cell cycle. Oncogene. 2008; 27:1905–1915. [PubMed: 17906696]

Welcker M, Orian A, Jin J, Grim JE, Harper JW, Eisenman RN, et al. The Fbw7 tumor suppressor regulates glycogen synthase kinase 3 phosphorylation-dependent c-Myc protein degradation. Proc Natl Acad Sci USA. 2004; 101:9085–9090. [PubMed: 15150404]

Wu CH, van Riggelen J, Yetil A, Fan AC, Bachireddy P, Felsher DW. Cellular senescence is an important mechanism of tumor regression upon c-Myc inactivation. (2007). Proc Natl Acad Sci USA. 2007; 104:13028–13033. [PubMed: 17664422]

Zhuang D, Mannava S, Grachtchouk V, Tang WH, Patil S, Wawrzyniak JA, et al. C-MYC overexpression is required for continuous suppression of oncogene-induced senescence in melanoma cells. Oncogene. 2008; 27:6623–6634. [PubMed: 18679422]

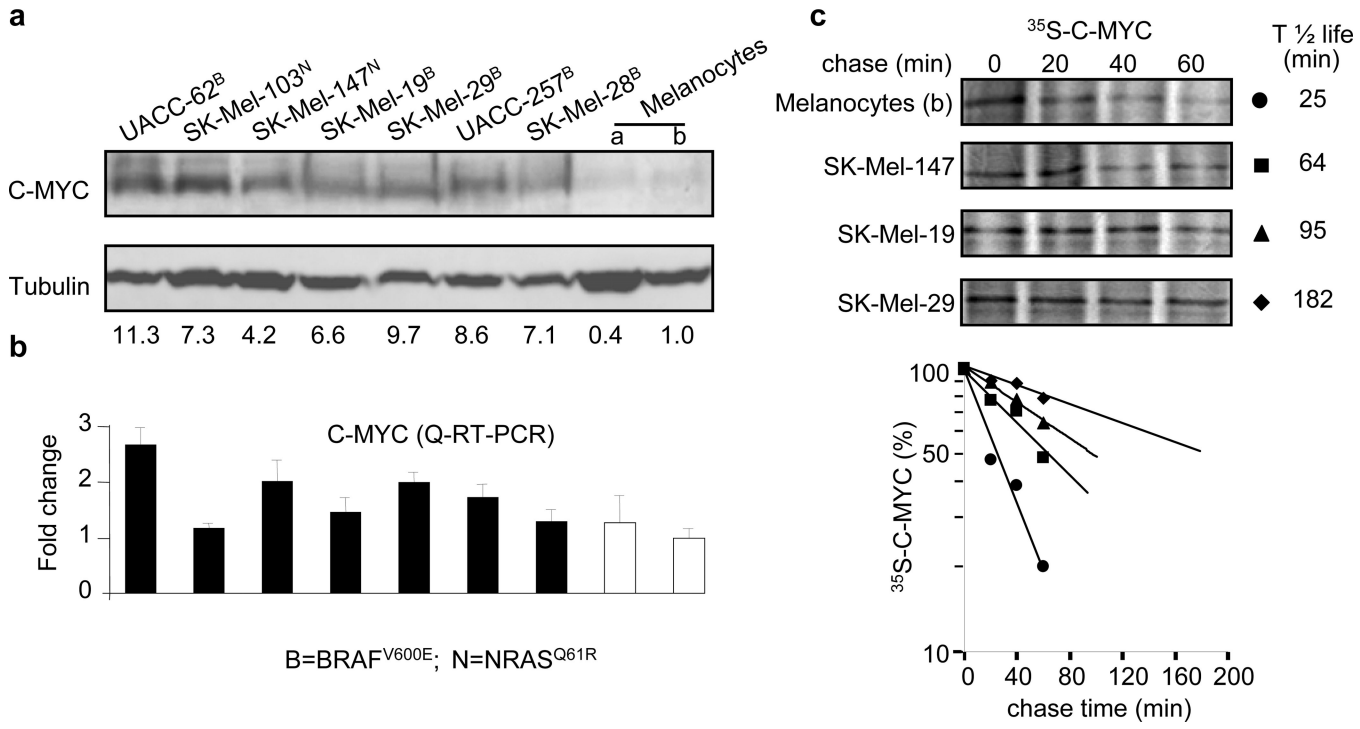

Figure 1. C-MYC in melanoma cells is controlled at the level of protein stability

(a) Total cellular extracts from two independently isolated populations of normal human melanocytes and indicated melanoma cell lines were probed by Western blotting with antibodies designated on the left. Numbers below the panels show the fold increase of C-MYC/tubulin ratio compared to that in the lane b (melanocytes).

(b) C-MYC/β-actin Q-RT-PCR signal ratios were obtained from total cellular RNAs corresponding to each cell line or population designated in (a). Signal ratios were normalized by the corresponding ratio in lane b (melanocytes).

(c) NHM and indicated melanoma cells were incubated with the mixture of ^{35}S-methionine/^{35}S-cysteine (300μCi/ml, Perkin-Elmer) in the cysteine/methionine-free media for 3 hours and 1 hour, respectively, for 0, 20, 40 or 60 minutes. After completion of incubation, cells were lysed and total cellular extracts were immunoprecipitated with mouse anti-C-MYC antibodies. Immunoprecipitated materials were separated on 10% SDS-PAGE, and labeled C-MYC was quantified using STORM phospho-imager. After background subtraction, band intensity was plotted on a log scale for each time point using Microsoft Excel graphing function, and C-MYC half-life was determined from the graph.

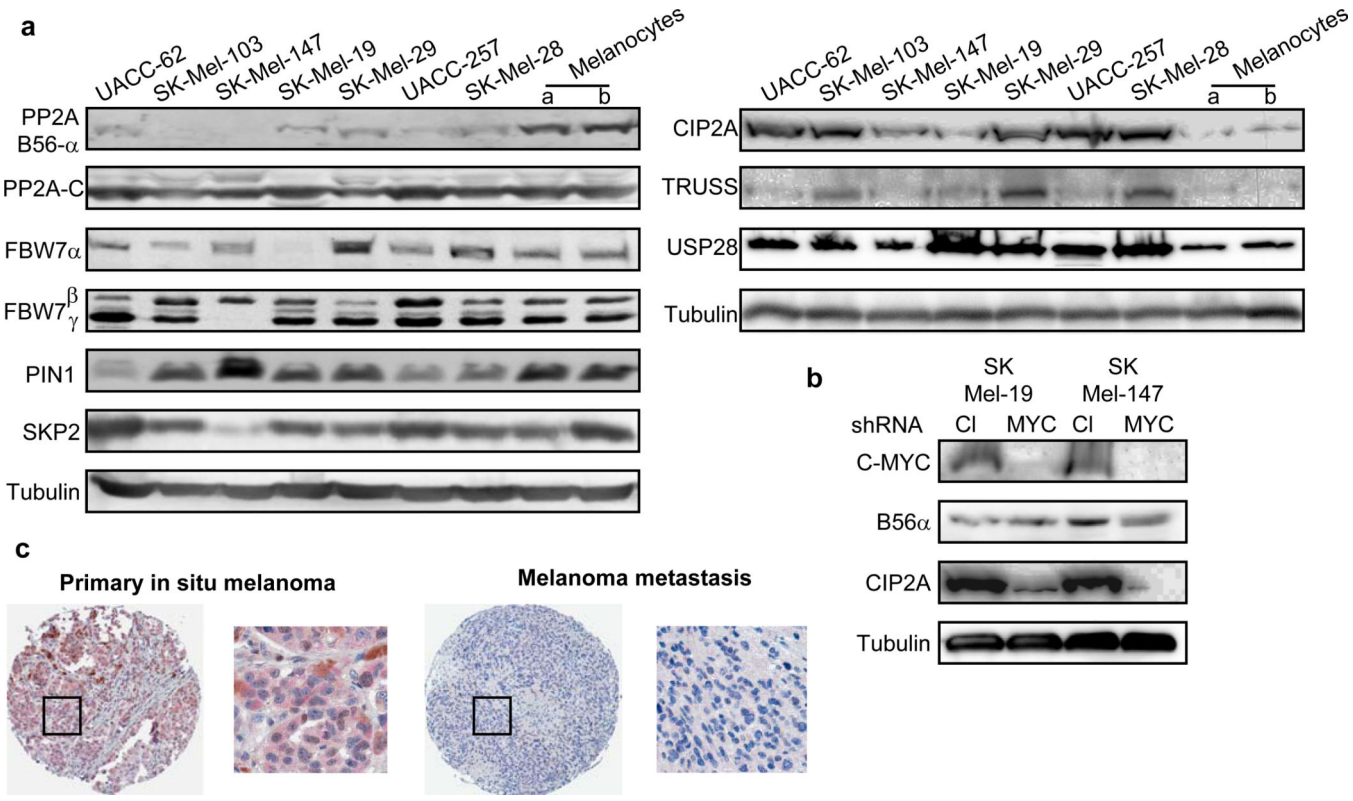

Figure 2. PP2A-B56α levels are suppressed in melanoma cells

(a) Total cellular extracts from two independently isolated populations of normal melanocytes and 7 melanoma cell lines were probed by Western blotting with antibodies designated on the left.

(b) Cells from indicated lines were infected with lentiviral vector expressing previously described C-MYC shRNA (M1, Wang et al, 2008) or with control vector. Cells were collected 5 days post-infection and total cellular extracts were probed by Western blotting with antibodies designated on the left.

(c) Representative examples of cores with highest PP2A-B56α staining (intensity score 3; more than 50% of cells stained) and lowest PP2A-B56α staining (intensity score 0) included in tissue microarrays. Shown below are higher-magnification views of the indicated areas. PP2A-B56α staining is cytoplasmic.

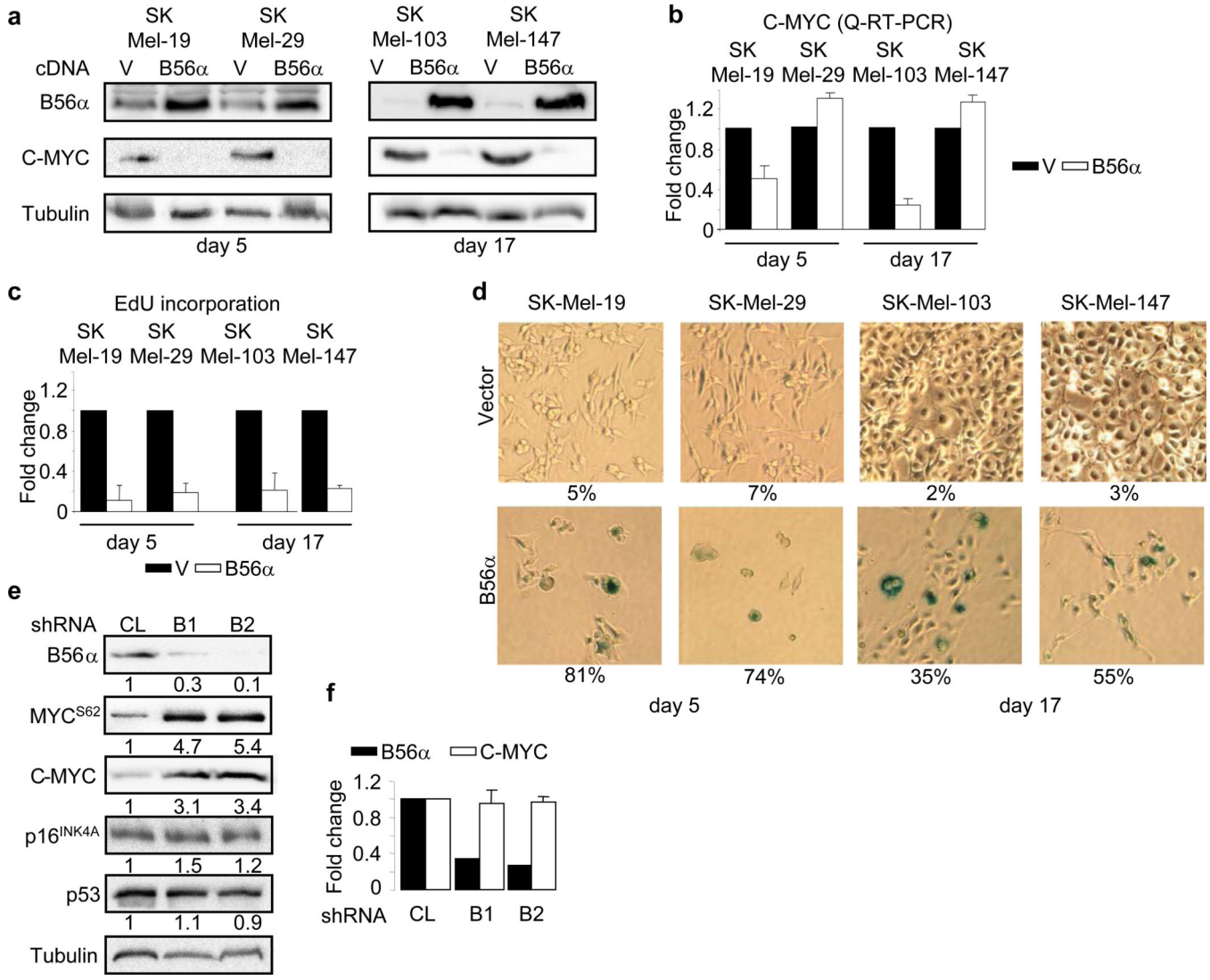

Figure 3. PP2A-B56α controls C-MYC protein levels in NHM and melanoma cells

(a) Cells from the indicated lines were infected with lentiviral vector expressing PP2A-B56α cDNA or with control vector and collected 5 or 17 days post-infection. Total cellular extracts were probed by Western blotting with antibodies designated on the left.

(b) Total RNAs collected from melanoma cells described in (a) were used in Q-RT-PCR to determine the C-MYC/β-actin mRNAs ratios; these ratios were normalized by the ratio obtained for cells infected with empty vector "V".

(c) Melanoma cells treated as in (a) were assayed for proliferation rates using EdU incorporation. Number of positive cells was divided by the number of total cells and normalized by the same ratio for cells expressing empty vector "V".

(d) Melanoma cells were infected as in (a). Cells were fixed and stained for SA-β-Gal activity 5 or 17 days after infection. Numbers below the panels correspond to the percent of SA-β-Gal-positive cells detected in each population by counting 100 cells (representative pictures are shown).

(e) NHM were infected in parallel with two independent shRNAs against PP2A-B56α gene (B1 or B2) or with control shRNA vector (CL). Cells were collected 5 days post-infection and total protein extracts were probed in Western blotting with the antibodies designated on the left. Numbers below the panels show the ratios of the corresponding protein to tubulin normalized by that ratio in control lane (CL).

(f) Total cellular RNAs were isolated from the cells described in (a). C-MYC/β-actin and PP2A-B56α/β-actin Q-RT-PCR signal ratios corresponding to each cell population were normalized by the corresponding ratio in control cells (CL).

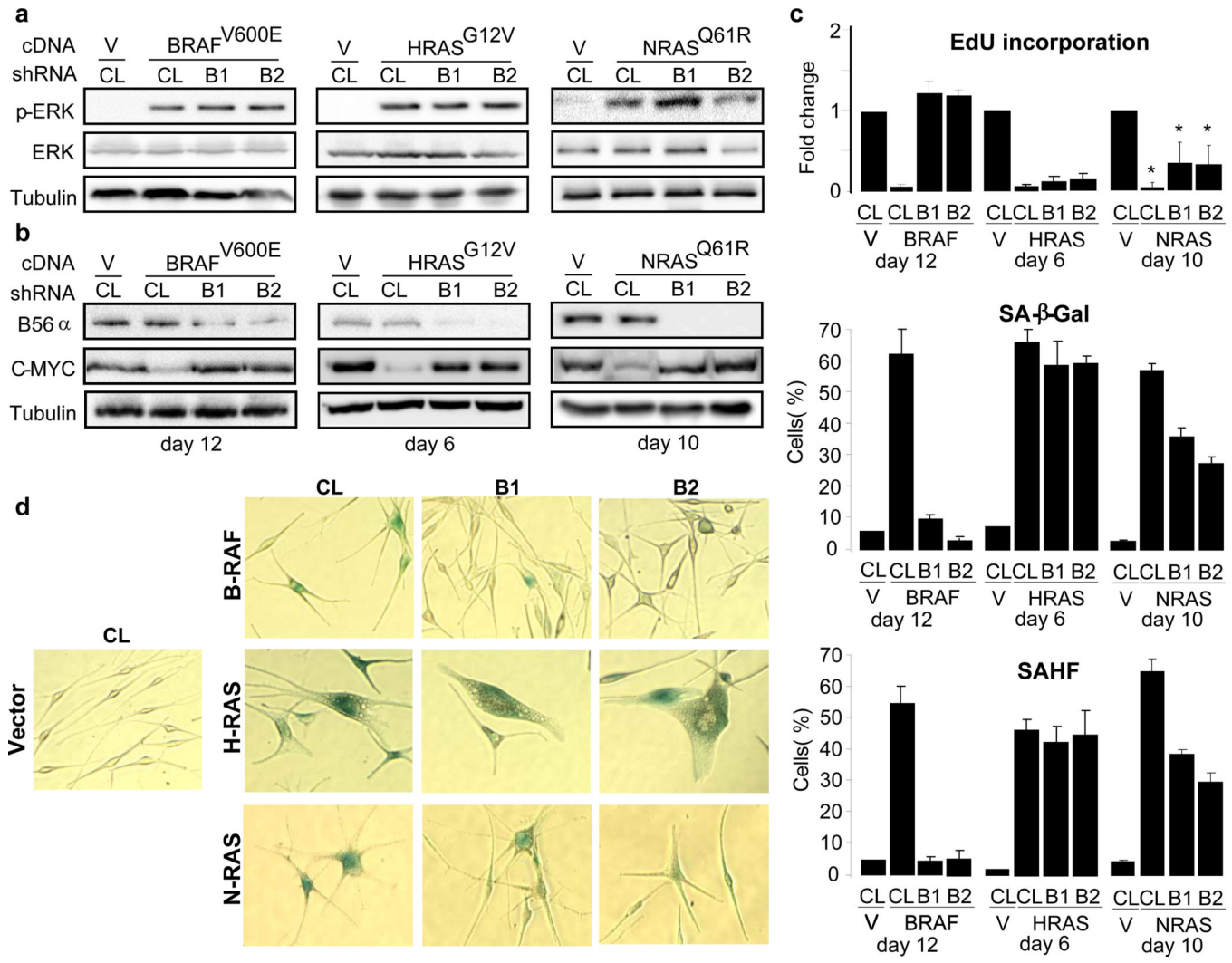

Figure 4. Depletion of PP2A-B56α differentially suppresses OIS caused by BRAF^{V600E}, NRAS^{Q61R} or HRAS^{G12V}

(a) NHM were infected with control lentiviral vector or vector expressing BRAF^{V600E}, HRAS^{G12V} or NRAS^{Q61R} cDNAs. Cells were collected 3 days post-infection and total protein extracts were probed in Western blotting with the antibodies designated on the left.

(b) NHMs were infected with control lentiviral vector or vector expressing BRAF^{V600E} cDNAs, followed by super-infection with control or PP2A-B56α shRNAs 3 days after the first infection. Cells were collected 12 days post second infection and total protein extracts were probed in Western blotting with the antibodies designated on the left; In parallel, NHM were infected with control or PP2A-B56α shRNAs followed by super-infection with control lentiviral vector or vectors expressing HRAS^{G12V} or NRAS^{Q61R} cDNA 4 days after the first infection. Cells were collected 6 days post second infection and total protein extracts were probed in Western blotting with the antibodies designated on the left.

(c) At the indicated time points, NHM infected like in (b), were assayed for proliferation rates (EdU incorporation), or fixed and stained for SA-β-galactosidase activity (SA-β-Gal) or stained with DAPI to visualize senescence-associated heterochromatin foci (SAHF). For

"EdU incorporation" number of positive cells was divided by the number of total cells and by the ratio of positive/total cells in control populations (CL/V). Asterisks indicate statistically significant difference between values corresponding to CL/NRAS and B1/NRAS ($p= 0.0433$) or CL/NRAS and B2/NRAS ($p= 0.0361$). For "SA-β-Gal", and "SAHF" the non-normalized percentage of cells is shown.

(d) NHM infected with the designated lentiviral vectors were fixed and stained for SA-β-galactosidase activity as described above (representative pictures are shown).

Table 1

Distribution of PP2A-B56α intensity scores in TMA cores from individuals with primary or metastatic melanomas

Tumor Stage	Intensity score			
	0	1	2	3
Primary	3	36	13	4
Metastatic	35	98	33	1

Staining intensity scores are as follows: no staining (0), weak staining (1), moderate staining (2), strong staining (3).